Scientific Papers. Series E. Land Reclamation, Earth Observation & Surveying, Environmental Engineering. Vol. X, 2021
Print ISSN 2285-6064, CD-ROM ISSN 2285-6072, Online ISSN 2393-5138, ISSN-L 2285-6064

MODEL OF DESCRIBING THE DIVING PHENOMENON AND THE DIVING DISTANCE OF THE LAND UNDER THE INFLUENCE OF MINING ACTIVITY. CASE STUDY JIU VALLEY, ROMANIA

Mihai Valentin HERBEI[1], Roxana Claudia HERBEI[2]
Florin SALA[1]

[1]Banat's University of Agricultural Sciences and Veterinary Medicine "King Michael Ist of Romania", 119 Aradului Street, Timisoara, Romania
[2]University of Petrosani, Mining Surveying and Real Estate, 20 University Street, Petrosani, Romania

Corresponding author email: florin_sala@usab-tm.ro

Abstract

The study analysed the phenomenon of diving (Div) and the diving distance (DivD) of the land under the influence of coal mining in the specific conditions of the Jiu Valley, Romania. 16 control points (CP1 to CP16) placed randomly on the study area were used. Measurements of control point coordinates (X, Y, Z coordinates) were made at a reference time (t_0) and at an interval of 3 months (t_1). ANOVA test confirmed the statistical safety of the data and the presence of variance in the data set ($p \leq 0.001$, F>>Fcrit, for Alpha = 0.001). The variation of the Div parameter according to Z_1 and Z_0 was described, in general conditions of statistical safety at the level of R^2 = 0.999; $p \leq 0.001$. The variation of the Div phenomenon according to X_0 and Z_0 was described under reduced statistical safety conditions ($p = 0.895$). The variation of DivD according to Z_1 and Z_0 was described in statistical safety conditions at the level of $R^2 = 0.697$, $p = 0.0142$, and according to X_0 and Z_0 it was described in statistical safety conditions at the level of $R^2 = 0.722$, $p = 0.0095$. The cluster analysis led to the grouping of control points based on affinity, in relation to the values Div and DivD, in statistical safety conditions (Coph.corr = 0.850).

Key words: *3D model, diving, diving distance, isoquant,t mining area.*

INTRODUCTION

The underground mining, the coal mining or the mining for various ores, generate a number of side effects on the environment, topography and quality of natural and agricultural land, human habitats and human health (Banash et al., 2016; Garci-Gomez & Perez-Cebada, 2020; Lechner et al., 2014; Schueler et al., 2011). Among the effects of underground mining operations can be mentioned the displacement and deformation of the lands following the exploitation of the useful mineral substance.

The different models have been developed for the study of objectives of interest, measurements and evaluation of spatio-temporal variation of surfaces (Bhattacharjee et al., 2020; Leibovici et al., 2020; Merciu & Paunescu, 2013; NourEldeen et al., 2020; Paunescu et al., 2015; Scaunas et al., 2019).

The need for underground resources obtained through mining and the negative impact of these operations already recorded, has led some studies to address issues for the sustainability of mining for the future (Sahu et al., 2015). In this context, there were introduced some concepts such as "ecological mining" respective "intelligent coal mining" (Wang et al., 2019; Wang et al., 2016).

The surfaces of the lands affected by the underground exploitations need to be monitored in time in order to know their dynamics and to take measures to protect the surfaces, the natural and anthropized ecosystems, as well as the existing constructions on them (Abaidoo et al., 2019; Dlamini & Xului, 2019; Ren et al., 2019). It is also necessary and very useful to forecast the phenomena that affect over time the areas in the mining perimeters, in order to sustainably develop these areas, these being generally mono-industrial and disadvantaged areas (Carvalho, 2017; Dubiński, 2013; Que et al., 2018; Segerstedt & Abrahamsson, 2019; Segura-Salazar & Tavares, 2018).

The ecosystems affected by coal mining have the ability to recover naturally, and the phenomenon of natural restoration has been recorded in various regions around the world (Cui et al., 2019).

Some studies have evaluated methods of bioremediation of areas affected by mining activities, especially in relation to heavy metals, by establishing and optimizing mixtures of tree species (Gorman et al., 2001; Samara et al., 2020).

From the analysis of a number of articles, that addressed the subject of mining, it was found increasing interest in addressing issues related to this sector, a low interdisciplinary, intersectorial and international interdisciplinary approach, but also the formation of trans-continental clusters in more collaborative countries, which indicated the need for research collaboration for solutions in sustainable mining (Bemke-Świtilnik et al., 2020).

To assess the impact of mining on land surface morphology, certain models were used that took into account parameters such as land slope, slope gradient, slope type, but also other parameters capable of capturing small variations in land (Ning et al., 2019).

Based on satellite technologies, some studies have evaluated the impact of mining on the environment using remote sensing and GIS (Bian et al., 2011; Padmanaban et al., 2017; Paull et al., 2008; Rudke et al., 2020).

In the context of these aspects, the present study analysed an area affected by underground coal mining operations and proposed models for assessing the diving and diving distance of the land in relation to the X, Y, Z reference coordinates of some control points.

MATERIALS AND METHODS

Based on the X, Y, Z reference coordinates and the regression analysis, the study proposed models to describe the phenomenon of landslide as a side effect associated with coal mining activities. The study area was located in the Jiu Valley, Romania (Figure 1), on a representative surface of 95,403.89 ha.

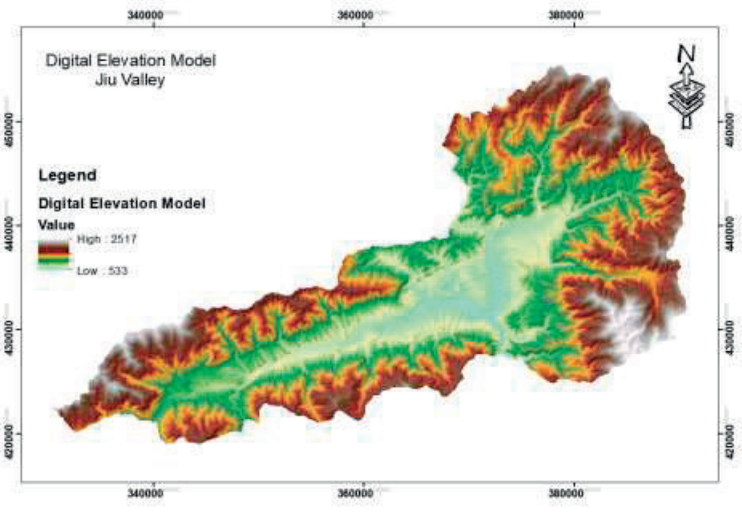

Figure 1. Map of digital elevation model, Jiu Valley, Romania

Land diving (Div) and diving distance (DivD) were assessed. To monitor the study area, 16 control points were established (PC1 to PC16), placed randomly on the surface of the affected land and taken into study.

For each control point, the reference coordinates (X, Y, X) were measured in the national projection system, Stereographic 1970, using GNSS satellite technologies, at two different times, t_0 as the initial moment and a moment t_1 at an interval of 3 months.

Diving is a vertical component of the displacement vectors, of the points located at the ground surface, in the diving bed. As a theoretical model, the point P (Figure 2) was considered to have moved during the period of influence in the P' position, along a curvilinear trajectory.

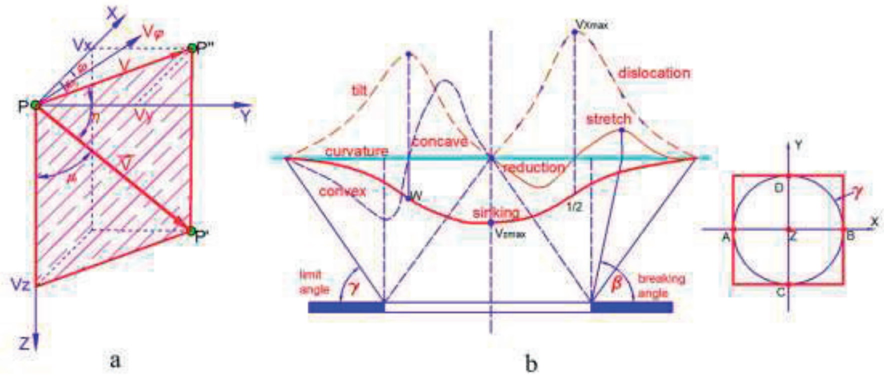

Figure 2. Scheme of principle for moving a point - a; The components of the ground surface movement above a critical extracted area: vertical components, horizontal components, plan view of the critical area - b

The line segment joining the starting point P with the end position P' defines the displacement vector V in a system of three-dimensional axes X, Y, Z, with the angle of inclination η and the orientation φ_0. This spatial vector can be projected on the horizontal plane XY obtaining the size of the horizontal displacement v and can be decomposed and analysed on the components VZ (immersion), VX and VY.

In other words, diving is the lowering of the surface area of the area in relation to the initial level of the same area, according to relation (1).

$$Div_i = H_i^* - H_i \quad (1)$$

where: Div - Diving the ground; H_i^* - height of the landmark at zero measurement; H_i - height of the current landmark.

It is necessary that the surface immersion be determined by topographic measurements of geometric-geodetic levelling. An observation mark is considered to be stable from a level point of view if its final immersion is less than 20 mm.

The horizontal movement (D_i^*) represents the horizontal component of point displacement vectors. It is the horizontal displacement of a point relative to its precedent, located in the area of influence of the operation. It is determined by the difference between the current distance and the same distance initially measured (before the sinking phenomenon), respectively:

$$D_i^* = D_{i,i+1} - D_{0i,i+1} \quad (2)$$

where: $D_{i,i+1}$ - the horizontal distance between the two marks on the current measurement;

$D_{0i,i+1}$ - the horizontal distance between the same two marks at the "zero" measurement.

The experimental data processing was done by ANOVA test, regression analysis, PCA and Cluster analysis. Parameters p, R^2, Coph. corr were used to express the statistical safety of the experimental data. ArcGis software was used to take over the data acquired from the field and to develop the DEM. PAST software (Hammer et al., 2001), mathematical module from EXCEL, and the Wolfram Alpha soft (Wolfram Research, 2020), were used for statistical analysis of the data.

RESULTS AND DISCUSSIONS

For the analysis and evaluation of the diving phenomenon in the study area, measurements were made in 16 control points for which the X, Y, Z coordinates were measured using GNSS satellite technology.

The data on the elevations at two different measurement moments (t_0 - initial reference moment and t_1 - evaluation moment), as well as the values for land diving (Div) and diving distance (DivD) are presented in Table 1.

The ANOVA test confirmed the safety of the data and the presence of variance in the data set collected in the study ($p \leq 0.001$, F>>Fcrit, for Alpha = 0.001).

Table 1. The experimental data regarding the slope of the land, Jiu Valley

PC	Current measurement (t_1)			Reference measurement (t_0)			Diving parameters	
	Northing X_1	Easting Y_1	Z_1	Northing X_0	Easting Y_0	Z_0	Diving the ground (mm/m)	Diving distance (m)
PC1	375545.4	436724.4	753.2381	375545.44	436724.37	753.2509	12.80	0.00
PC2	375561	436735.4	751.926	375560.99	436735.44	751.9441	18.10	19.090
PC3	375156.5	436244.8	824.3654	375156.46	436244.86	824.442	76.60	635.860
PC4	375145.3	436247.6	823.6287	375145.25	436247.61	823.7567	128.00	11.534
PC5	375083.1	436036.5	773.9746	375083.13	436036.56	773.0532	-921.40	220.002
PC6	374894.3	435984	752.8033	374894.34	435984.04	752.8398	36.50	195.967
PC7	375829.6	435197.4	824.734	375829.65	435197.41	824.7341	0.10	1222.123
PC8	375838.1	435229	824.2524	375838.1	435229	824.3261	73.70	32.702
PC9	374007.4	436017.2	647.994	374007.43	436017.22	648.0599	65.90	1993.150
PC10	373716.7	436636.2	687.221	373716.73	436636.18	687.2205	-0.50	683.830
PC11	373708.6	436587	679.6566	373708.63	436586.99	679.6912	34.60	49.855
PC12	375014.9	436186.5	806.1427	375014.94	436186.49	806.2434	100.70	1366.326
PC13	375442.8	436121.3	830.6045	375442.8	436121.26	830.6333	28.80	432.802
PC14	375828.1	436275.2	775.8731	375828.09	436275.2	775.8539	-19.20	414.906
PC15	374418.6	435822.4	676.3189	374418.57	435822.45	676.3487	29.80	1480.448
PC16	375185.1	436083.8	786.0972	375185.15	436083.77	786.1562	59.00	809.898

A digital model of the study area is presented in Figure 3. The graphical distribution of the terrain diving in relation to the diving distance, based on the measured values, is presented in Figure 4, and real images from the terrain are shown in Figure 5.

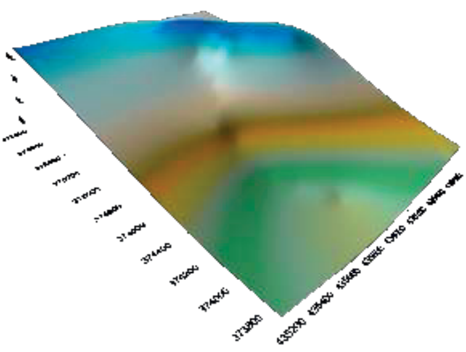

Figure 3. Digital model of the studied area

Considering the overall appearance of the area under study, and the variation of the values recorded for diving and the diving distance of the land under specific conditions in the Jiu Valley, Romania, an analysis was made of the variance of these elements (Div, DivD) in the report with the values of the elevations of the 16 control points (PC1 to PC16).

Multiple regression analysis was used which analysed the variation of the studied elements Div and DivD depending on the elevations of the control points at the reading times t_0 and t_1.

Based on this analysis, models of variation of Div and DivD were found, in statistical safety conditions only in relation to X_0, Z_0 and Z_1. The models found were of the form f (X_0, Z_0) and f (Z_1, Z_0). The variation of the Div parameter according to Z_1 and Z_0 was described by equation (3), in general conditions of statistical safety (R^2 = 0.999; $p \leq 0.001$).

Print ISSN 2285-6064, CD-ROM ISSN 2285-6072, Online ISSN 2393-5138, ISSN-L 2285-6064

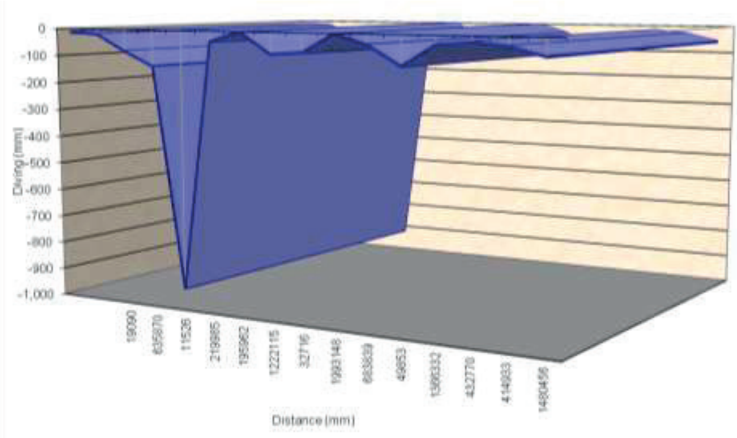

Figure 4. The diving and the diving distance of the land in the study area, Jiu Valley

Figure 5. Images of the diving process in the studied area, Jiu Valley, Romania

The 3D graphic representation is shown in Figure 6, and the isoquant graphic representation is presented in Figure 7.

$$Div = ax^2 + by^2 + cx + dy + exy + f \qquad (3)$$

where: x - Z_1;

y - Z_0;

a, b, c, d, e, f - coefficients* of the equation (3);

a = -6.56289;

b = -6.50970;

c = -999.99998;

d = 999.99998;

e = 1.30726;

f = 0.

*For high accuracy, the values of the coefficients of equations were 16 decimal digits.

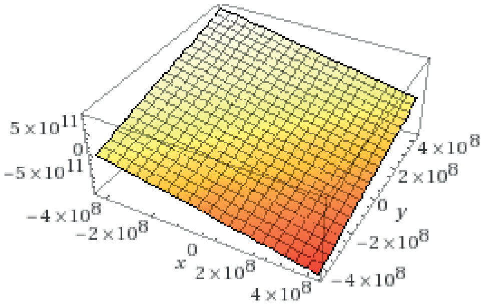

Figure 6. The 3D graphic representation of the Div variation in relation to the Z_1 (x-axis) and Z_0 (y-axis) elevations of the land in the study area

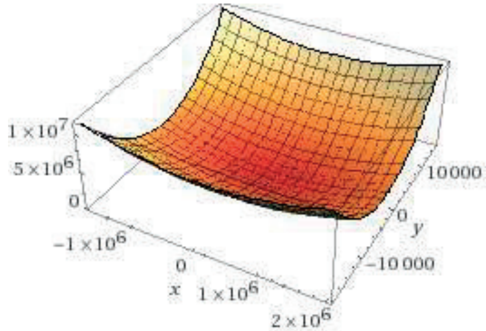

Figure 8. 3D graphic representation of the Div variation in relation to X_0 (x-axis) and Z_0 (y-axis) of the field in the study area

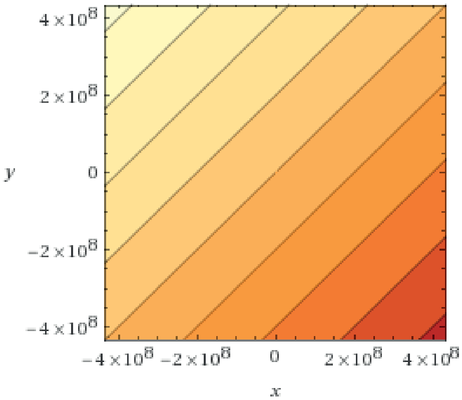

Figure 7. Isoquant distribution of Div values as a function of Z_1 (x-axis) and Z_0 (y-axis) in the study area

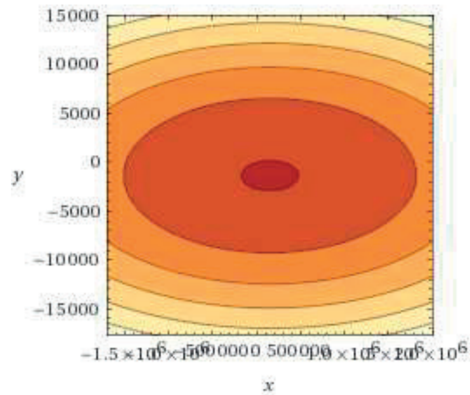

Figure 9. The isoquant distribution of Div values as a function of X_0 (x-axis) and Z_0 (y-axis)

The variation of the Div parameter according to X_0 and Z_0 was described by equation (4), under reduced statistical safety conditions (p = 0.895). The 3D graphical representation is shown in Figure 8, and the graphical representation in the form of isoquants is shown in Figure 9. Similar results for the Div variation were obtained in relation to the values X_0 and Z_1.

$$Div = ax^2 + by^2 + cx + dy + exy + f \tag{4}$$

where: x - X_0;

y - Z_0;

a, b, c, d, e, f - coefficients of the equation (4);

a = 7.47012;

b = 0.03307;

c = -0.23027;

d = 90.39512;

e = -0.00037;

f = 0.

Similarly, multiple regressions were used to find the variation of the diving distance (DivD) depending on the values of the X and Z elevations. Equation (5) resulted which described in statistical safety conditions (R^2 = 0.697, p = 0.0142) the DivD variation depending on Z_1 and Z_0. The 3D graphical distribution is shown in Figure 10. Based on equation (5), the optimal values for x (Z_1) and y (Z_0) were found in the amount of and for x_{opt} = 805.0131243, and y_{opt} = 805.0387029. The graphical distribution in the form of isoquants is shown in Figure 11. In relation to these values x (Z_1) and y (Z_0) found for the DivD variation, between the control points 10 were positioned with lower values (PC16, PC14, PC5, PC1, PC6, PC2, PC10, PC11, PC15, PC9, in descending order), and 6 with higher values (PC13, PC7, PC3, PC8, PC4, PC12, in descending order).

$$\mathrm{DivD} = ax^2 + by^2 + cx + dy + exy + f \quad (5)$$

where: x - Z_1;
y - Z_0;
a, b, c, d, e, f - coefficients of the equation (5);
a = 5681.51674;
b = 5501.25820;
c = -144828.33875;
d = 144825.18381;
e = -11182.77013;
f = 0.

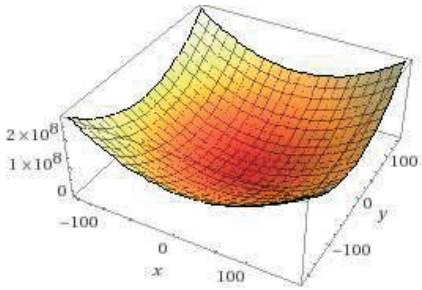

Figure 10. The 3D graphic representation of the DivD variation in relation to the Z_1 (x-axes) and Z_0 (y-axes) elevations of the land in the study area

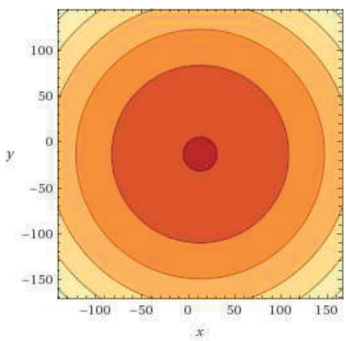

Figure 11. The isoquant distribution of DivD values according to Z_1 (x-axes) and Z_0 (y-axes)

Regarding the variation of DivD as a function of X_0 and Z_0, the multiple regression analysis led to equation (6) in statistical safety conditions ($R^2 = 0.722$, $p = 0.00952$). The 3D graphical distribution is shown in Figure 12. From the analysis of the values but also of the 3D graphical distribution, it was found that under the study conditions, the DivD variation in relation to X_0 and Z_0 was very strongly influenced by the Z_0 quota (y-axis) for which the optimal value $y_{opt} = 777.24169$ was found. Under the same conditions, the contribution of the X_0 quota (x-axis) to the DivD variation was reduced. The distribution of the graph in the form of isoquants is shown in Figure 13.

$$\mathrm{DivD} = ax^2 + by^2 + cx + dy + exy + f \quad (6)$$

where: x - X_0;
y - Z_0;
a, b, c, d, e, f - coefficients of the equation (6);
a = 0.000017;
b = 0.18259;
c = -5.99179;
d = 2894.59422;
e = -0.00846;
f = 0.

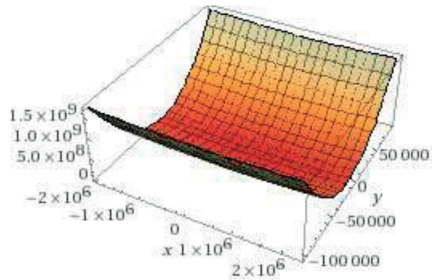

Figure 12. The 3D graphic representation of the DivD variation in relation to the X_0 (x-axes) and Z_0 (y-axes) elevations of the land in the study area

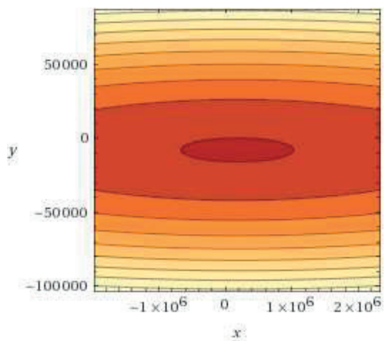

Figure 13. The isoquant distribution of DivD values as a function of X_0 (x-axes) and Z_0 (y-axes)

The cluster analysis led to the grouping of control points based on affinity, in relation to the Div and DivD values, in statistical safety conditions (Coph.corr = 0.850), Figure 14.
The control points were found to be grouped into two distinct clusters C1 (12 control points) and C2 (4 control points), with several subclusters each. A high degree of similarity in terms of Div and DivD was found in CP1

and CP2, CP8 and CP11 (these five control points having the common root in the cluster structure, C1 cluster), respectively CP13 and CP14.

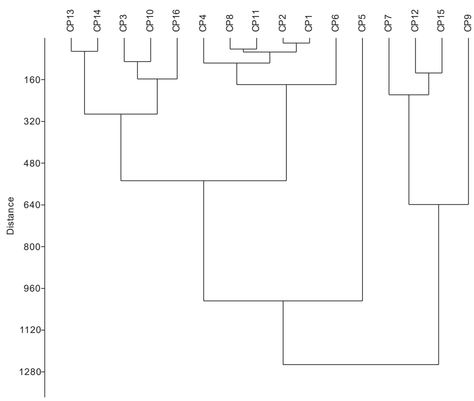

Figure 14. The dendrogram for grouping control points in relation to Div and DivD based on Euclidean distances

The natural, agricultural or urban areas are studied by remote sensing and imaging analysis from the perspective of natural resources assessment, environmental monitoring and quality of life conditions, farm management, so that numerous studies have addressed such topics and provided information, models and methods. (Govedarica et al., 2016; Popescu et al., 2020; Sala et al., 2020). The lands affected by the mining activities acquire in time an ecological stability in natural conditions (Zipper et al., 2011). Some studies have confirmed a direct relationship between the content of some mineral elements in the rock and substrate (e.g. K) and the volume of the trees (Wang et al., 2016). At the same time, such areas can be ecologically rehabilitated through tree plantations to consolidate the land (Weijer, 2019; Corrêa et al., 2018; Macdonald et al., 2015). Plantations of fruit trees, vines (local germplasm is recommended for adaptability and high resistance), or agricultural crops can be set up according to specific conditions, being promoted alternative technologies and different optimization models (Dobrei et al., 2015; Sala and Boldea, 2011). Also, some studies have addressed aspects of urban development and quality of life in areas where mining predominates, especially coal, these areas being generally mono-industrial areas and disadvantaged areas (Oncia et al., 2013a; Obiri et al., 2016; Oncia et al., 2013b;).

The secondary influence of mining activities on the distribution of post-mining permeability and water regime in the respective basins was studied based on numerical models and permeability functions (Fan et al., 2020).

“Post-mining” areas were evaluated through different scenarios in relation to the depth of subsidence and integrated models of simulation and optimization of their use structure in relation to the landscape structure, ecological benefits, agricultural land area, urban or industrial development (Li et al., 2020).

Some studies that have considered the promotion of ecological mining have proposed models that have integrated as actors both mining companies and the local administration and that have taken into account various factors on the choice of exploitation (Zhao et al., 2020).

The present study described the phenomenon of diving and the distance of land diving as a side effect of coal mining in the Jiu Valley, Romania.

The diving phenomenon represents the vertical component (Z) and in relation to the values Z_1 (time t_1) and Z_0 (time t_0) of the control points the diving process was described most accurately, $R^2 = 0.999$, $p << 0.001$, equation (3). When X values were taken alongside the Z values, the estimation accuracy of Div decreased ($p = 0.895$), equation (4). However, the 3D model, Figure 7, showed that the variation of the Z values (y-axis, in the graph) has great significance in the description of the diving phenomenon (Div).

The description of the diving distance (DivD) based on the values Z_1 and Z_0, equation (5), was made in low safety conditions ($R^2 = 0.697$, $p = 0.014$), which confirms that the Z values are closely associated with the vertical component, so with the diving process, not with the diving distance, for which the values X and Y are necessary.

In the context of the presented aspects, the present study evaluated the diving phenomenon and the diving distance and proposed models to describe this phenomenon in the concrete conditions of the Jiu Valley, Romania.

CONCLUSIONS

The diving phenomenon and the diving distance of the land under the influence of mining operations in the Jiu Valley, Romania, was analysed based on coordinate values in the Stereographic 1970 projection system of 16 control points, as current determinations (t_1) compared to a reference moment (t_0).
Diving (Div) and diving distance (DivD) were described by mathematical models according to the values of X, Y, Z coordinates. 3D and isoquant distributions of the diving variation were obtained according to the values X_0, Z_0 and Z_1, as graphical models of behaviour of the analysed phenomena.
Z-values are recommended for models that describe the diving phenomenon (vertical component of the process as a whole), and X and Y values are recommended in models for describing the direction of immersion of the ground.

REFERENCES

Abaidoo, C.A., Osei, E.M.Jnr., Arko-Adjei, A., Prah, B.E.K., 2019. Monitoring the extent of reclamation of small scale mining areas using Artificial Neural Networks, *Heliyon*, 5(4):e01445.

Bansah, K.J., Yalley, A.B., Dumakor-Dupey, N., 2016. The hazardous nature of small-scale underground mining in Ghana, *J. Sustain. Min*., 15(1):8-25.

Bemke-Świtilnik, M., Drabek, A., Kamińska, A.M., Smoliński, A., 2020. Research collaboration patterns in sustainable mining - A Co-authorship analysis of publications, *Sustainability*, 2020, 12(11):4756.

Bhattacharjee, S., Chen, J., Ghosh, S.K., 2020. Spatio-temporal prediction of land surface temperature using semantic kriging, *Transactions in GIS*, 24(1):189-212.

Bian, Z., Zhang, H., Lei, S., 2011. Analyses of environmental impacts of underground coal mining in an arid region using remote sensing and GIS, *J. Coal Sci. Eng. China*, 17:363-371.

Carvalho, F.P., 2017. Mining industry and sustainable development: time for change. *Food Energy Secur*.**,** 6(2):61-77.

Corrêa, R.S., Balduíno, A.P. do C., Teza, C.T.V., Baptista, G.M. de M., 2018. Vegetation cover development resulting from different restoration approaches of exploited mines, *Floresta e Ambient,* 25(4):e20171116.

Cui, X., Peng, S., Lines, L.R., Zhu, G., Hu, Z., Cui, F., 2019. Understanding the capability of an ecosystem nature-restoration in coal mined area, *Sci. Rep.*, 9:19690.

Dlamini, L.Z.D., Xulu, S., 2019. Monitoring mining disturbance and restoration over RBM Site in South Africa using LandTrendr algorithm and Landsat data, *Sustainability*, 11(24):6916.

Dobrei, A., Dobrei, A.G., Nistor, E., Iordanescu, O.A., Sala, F., 2015. Local grapevine germplasm from Western of Romania - An alternative to climate change and source of typicity and authenticity, Agric. *Agric. Sci. Proc*., 6:124-131.

Dubiński, J., 2013. Sustainable development of mining mineral resources, *J. Sustain. Min*., 12(1):1-6.

Fan, G., Zhang, S., Cao, B., Zhang, D., Zhang, C., 2020. Impact of mine panel size on hydraulic permeability of weakly cemented strata, *Sustainability*, 12(6):2396.

Garcia-Gómez, J.J., Pérez-Cebada, J.D., 2020. A socio-environmental history of a copper mining company: Rio-Tinto Company Limited (1874–1930), *Sustainability*, 12(11):4521.

Gorman, J., Skousen, J., Sencindiver, J., Ziemkiewicz, P., 2001. Forest productivity and minesoil development under a white pine plantation versus natural vegeta,tion after 30 years, In: *Proceedings, 18th Annual National Conference of the American Society of Mining and Reclamation, Lexington*, 103-111.

Govedarica, M., Ristic, A., Herbei, M.V., Sala, F., 2015. Object oriented image analysis in remote sensing of forest and vineyard areas, *Bulletin UASVM Horticulture*, 72(2):362-370.

Hammer, Ø., Harper, D.A.T., Ryan, P.D., 2001. PAST: Paleontological statistics software package for education and data analysis. *Palaeontol. Electron*. 4(1):1-9.

Lechner, A.M., Baumgartl, T., Matthew, P., Glenn, V., 2014. The impact of underground longwall mining on prime agricultural land: A review and research agenda, *Land Degrad. Dev*., 27(6):1650-1663.

Leibovici, D.G., Quegan, S., Comyn-Platt, E., Hayman, G., Martin, M.V., Guimberteau, M., Druel, A., Zhu, D., Ciais, P., 2020. Spatio-temporal variations and uncertainty in land surface modelling for high latitudes: univariate response analysis, *Biogeosciences*, 17:1821-1844.

Li, Z., Wu, S., Zhang, S., Nie, C., Li, Y., Huang, Y., 2020. Optimization of land reuse structure in coal mining subsided areas considering regional economic development: A case study in Pei County, China, *Sustainability*, 12(8):3335.

Macdonald, S.E., Landhäusser, S.M., Skousen, J., Franklin, J., Frouz, J., Hall, S., Jacobs, D.F., Quideau, S., 2015. Forest restoration following surface mining disturbance: challenges and solutions, *New Forests*, 46:703-732.

Merciu, G.L., Paunescu, C., 2013. Use of the Geographic Information System in locating and evaluating the conservation of historical district in the city of Resita, *J. Appl. Eng. Sci*., 16(2):63-70.

Ning, L., Zhao X.-G., Song S.-J., Zhou W.-F., 2019. Effect of underground coal mining on slope morphology and soil erosion, *Math. Probl. Eng*., 5285126.

NourEldeen, N., Mao, K.,Yuan, Z., Shen, X., Xu, T., Qin, Z., 2020. Analysis of the spatiotemporal change in land surface temperature for a long-term sequence in Africa (2003-2017), *Remote Sens.*, 12(3):488.

Obiri, S., Mattah, P.A., Mattah, M.M., Armah, F.A., Osae, S., Adu-kumi, S., Yeboah, P.O., 2016. Assessing the environmental and socio-economic impacts of artisanal gold mining on the livelihoods of communities in the Tarkwa Nsuaem Municipality in Ghana, *Int. J. Environ. Res. Public Health*, 13(2):160.

Oncia, S., Herbei, M., Popescu, C., 2013a. Study of territorial and infrastructure development in the Petrosani city - The Hunedoara county using GIS elements, *J. Environ. Prot. Ecol*., 14(1):225-232.

Oncia, S., Herbei, M., Popescu, C., 2013b. Sustainable development of the Petrosani City, the Hunedoara County based on GIS analysis, *J. Environ. Prot. Ecol.*, 14(3):232-240.

Padmanaban, R., Bhowmik, A.K., Cabral, P.A., 2017. Remote sensing approach to environmental monitoring in a reclaimed mine area, *Int. J. Geo-Inf.*, 6:401.

Paull, D., Banks, G., Ballard, C., Gillieson, D., 2008. Monitoring the environmental impact of mining in remote locations through remotely sensed data, *Geocarto Int*., 21(1):33-42.

Păunescu, C., Vasile, C., Ciuculescu, C., 2015. Considerations for GNSS measurements. *RevCAD Journal of Geodesy and Cadastre*, 18:5-13.

Popescu, C.A., Herbei, M.V., Sala, F., 2020. Remote sensing in the analysis and characterization of spatial variability of the territory. A study case in Timis County, Romania, *Scientific Papers Series Management, Economic Engineering in Agriculture and Rural Development*, 20(1):505-514.

Que, S., Wang, L., Awuah-Offei, K., Chen, Y., Yang, W., 2018. The status of the local community in mining sustainable development beyond the triple bottom line, *Sustainability*, 10:1749.

Ren, H., Zhao, Y., Xiao, W., Hu, Z., 2019. A review of UAV monitoring in mining areas: current status and future perspectives, *Int. J. Coal. Sci. Technol*., 6:320-333.

Rudke, A.P., Souza, V.A.S.De., Santos, A.M.Dos., Xavier, A.C.F., Filho, O.C.R., Martins, J.A., 2020. Impact of mining activities on areas of environmental protection in the southwest of the Amazon: A GIS- and remote sensing-based assessment, *J. Environ. Manage*., 263:110392.

Sahu, H.B., Prakash, N., Jayanthu, S., 2015. Underground mining for meeting environmental concerns - A strategic approach for sustainable mining in future, *Procedia Earth Planet. Sci*., 11:232-241.

Sala, F., Boldea, M., 2011. On the optimization of the doses of chemical fertilizers for crops, *AIP Conf. Proc.*, 1389:1297-1300.

Sala, F., Popescu, C.A., Herbei, M.V., Rujescu, C., 2020. Model of color parameters variation and correction in relation to "Time-View" image acquisition effects in wheat crop, *Sustainability*, 12(6):2470.

Samara, T., Spanos, I., Platis, P., Papachristou, T.G., 2020. Heavy metal retention by different forest species used for restoration of post-mining landscapes, N Greece, *Sustainability*, 12(11):4453.

Scaunas, S., Paunescu, C., Merciu, G.L., 2019. Spatial-temporal analysis of land cover and use changes using gis tools. Case study Băneasa neighborhood, Bucharest, *J. Appl. Eng. Sci*., 9(2):187-194.

Schueler, V., Kuemmerle, T., Schröder, H., 2011. Impacts of surface gold mining on land use systems in Western Ghana, *Ambio*, 40(5):528-539.

Segerstedt, E., Abrahamsson, L., 2019. Diversity of livelihoods and social sustainability in established mining communities, *The Extractive Industries and Society*, 6(2):610-619.

Segura-Salazar, J., Tavares, L.M., 2018. Sustainability in the minerals industry: Seeking a consensus on its meaning, *Sustainability*, 10:1429.

Wang, J., Wang, H., Cao, Y., Bai, Z., Qin, Q., 2016. Effects of soil and topographic factors on vegetation restoration in opencast coal mine dumps located in a loess area, *Sci. Rep*. 6:22058.

Wang, G., Xu, Y., Ren, H., 2019. Intelligent and ecological coal mining as well as clean utilization technology in China: Review and prospects, *Int. J. Min. Sci. Technol*., 29(2):161-169.

Weijer, M.van de., 2019. Changing use and performance of industrial estates from 1965 onward: the case of the Parkstad conurbation, the Netherlands, *J. Urban Des*., 24(3):406-423.

Wolfram, 2020. Research, Inc., Mathematica, Version 12.1, Champaign, IL.

Zhao, Y., Zhao, G., Zhou, J., Pei, D., Liang, W., Qiu, J., 2020. What hinders the promotion of the green mining mode in China? A Game-Theoretical Analysis of local government and metal mining companies, *Sustainability*, 12(7):2991.

Zipper, C.E., Burger, J.A., Skousen, J.G., Angel, P.N., Barton, C.D., Davis, V., Franklin, J.A., 2011. Restoring forests and associated ecosystem services on Appalachian coal surface mines, *Environ. Manage.*, 47:751-765.